POWER INTERMITTENCY IN PEM ELECTROLYSERS DIRECTLY COUPLED WITH WIND PARKS: A CASE STUDY ON DYNAMIC STACK OPERATION IN NORTHERN BAVARIA

Petros Polykarpoulos*, Matthias Welzl, Dieter Brüggemann

Chair of Engineering Thermodynamics and Transport Processes (LTTT), Center of Energy Technology (ZET), University of Bayreuth, Germany

*Corresponding Author: Petros.Polykarpoulos@uni-bayreuth.de

ABSTRACT

Nowadays, the global demand for decentralised hydrogen production and autonomous grids is paving the way for electrolyser units directly coupled with renewable sources. However, the proposed grid-independent electrolyser configurations are subject to a significant level of intermittency, affecting their operation and degradation behaviour. In this paper, wind speed volatility is firstly characterised across the frequency range and synthetic wind speed profiles are generated for specific turbulence parameters. Using a low-order, transient wind turbine model, dynamic power output can be estimated for short wind signal intervals. It is underlined that wind turbine response can filter out the high-frequency components of wind speed fluctuations due to their inertial characteristics and the use of control systems. Furthermore, a methodology has been implemented to account for the smoothing effect on the aggregate power output of geographically dispersed turbines inside a wind park. The power-to-gas plant operating in the Wunsiedel Energy Park in Northern Bavaria, Germany, is examined as a case study, assuming a direct coupling of the electrolyser with a wind power source. Its dynamic behaviour is investigated for various wind power profiles, modular configurations (1, 2 or 4 independent modules), and electrolyser capacity (100 % or 50 % of the wind park rated power). All cases are evaluated in terms of energy utilisation and hydrogen production. It is demonstrated that the technical specifications of the electrolyser, in particular its operational range and warm startup time, strongly influence its load-following capability. A higher number of independent modules offers enhanced flexibility and energy utilisation for dynamic operation. Dimensioning the electrolyser at 50 % of the wind park rated power is proved to provide similar hydrogen production at lower wind speeds compared to the 100 % case.

1 INTRODUCTION

In recent years, there has been a growing interest in developing sustainable alternatives to the current fossil fuel-based energy economy to gradually achieve decarbonisation and mitigate the effects of global warming. The European Union has set itself the target of achieving net zero emissions by 2050 and at least 55% by 2030, through the European Green Deal (European Commission, 2019). Hydrogen is widely regarded as a promising energy carrier, due to its application versatility, ability to directly utilise renewable energy, and potential for long-term storage (Ajanovic *et al.,* 2024). Moreover, energy grids are currently not capable of integrating all the renewable energy production, resulting in a high amount of curtailment and thus hydrogen generation can potentially utilise this excess energy (Maggio *et al.*, 2019). Only in Germany, 5.8 GWh of renewable energy was curtailed in 2021, almost 95% of which attributed to onshore and offshore wind sources (Bundesnetzagentur, 2022).

Terlouw *et al.* (2022) categorised electrolyser configurations based on their connection status to the national grid: grid-connected, hybrid or autonomous. Grid connection provides backup supply when renewable energy is not sufficient and as a buffer against wind and solar intermittency. Autonomous configurations are necessary for special applications, such as remote island grids, but are also actively

https://doi.org/10.52202/077185-0072

promoted by legislative initiatives: The recently updated Renewable Energy Directive II (European Commission, 2023) defines a strict framework for the production of renewable fuels (including green hydrogen) in the European Union, setting restrictions on grid-connected hydrogen production, ensuring thus a low carbon footprint (Barreda, 2023).

Kojima *et al.* (2023) addressed the nature of wind and solar intermittency as well as its effects on coupled electrolyser systems, resulting in various degradation mechanisms among electrolyser technologies. Lange *et al.* (2023) reviewed the degree of flexibility of the most common electrolyser types according to their technical specifications as well as the impact of dividing the entire system into independent subsystems, or alternatively called modules. PEM electrolysers were indicated as more suitable for dynamic operation, while alkaline and solid oxide electrolysers as better suited for base operation. However, a study by Schnuelle *et al.* (2020) compared alkaline and PEM electrolysers under variable solar or wind load and showed that while PEM electrolysers achieved better energy utilisation, overall hydrogen production and efficiency were lower. Sarrias-Mena *et al.* (2015) simulated a PEM electrolyser using power input from a single wind turbine. They demonstrated how an electrolysis cell responds to load fluctuations and proved that voltage stability can be maintained during operation. Furthermore, Mucci *et al.* (2023) evaluated the operational flexibility of PEM electrolysers and downstream power-to-x processes for the production of e-fuels.

A number of studies have also assessed the optimal sizing of such electrolyser systems, based on the performance of their respective renewable sources. For instance, Egeland-Eriksen *et al.* (2023) suggested a hybrid, offshore wind park-electrolyser connection and showed the direct correlation between the capacity factor, the electricity price, and the plant productivity. Similarly, Hassan *et al.* (2023) investigated an alkaline water electrolyser coupled with either solar or wind power plants, estimating the optimal electrolyser capacity for each case, based on techno-economic criteria and including the carbon footprint. Hofrichter *et al.* (2023) proposed a methodology to determine the optimal electrolyser capacity, when coupled with solar or wind sources. Full load hours impact predominantly the sizing of an electrolyser, which might even reach 143% of an offshore wind plant nominal power. Additionally, Cooper *et al.* (2022) described the two-step optimisation of an electrolysis system coupled with a wind plant based on techno-economic criteria. Their analysis focused on the dimensioning of the electrolyser, considering combinations of stack number and size, electrolyser type (AEM or PEM), and pressure level.

Lastly, some studies focus on the performance optimisation of the electrolyser system under fluctuating operation. Lu *et al.* (2023) examined a wind-PEM electrolysis system under the scope of both efficiency and degradation, optimising its power allocation strategy. An important remark from this study is that an external power supply was used to maintain the minimum voltage to avoid frequent shutdowns that contribute to increased degradation and safety concerns. Fang and Liang (2019) researched a wind-hydrogen integrated system with an alkaline electrolyser and proposed the use of supercapacitors to overcome short term fluctuations and modular adaptive control strategies to maximise hydrogen production. Tully *et al.* (2023) simulated an electrolyser coupled with a fluctuating wind source, taking into consideration cumulative degradation. They proposed a framework to optimize electrolyser operation, based on policies concerning stack activation and power distribution.

This paper presents a novel framework for estimating dynamic load in electrolyser units directly powered by wind sources. The introduced methodology could contribute to dimensioning wind-electrolyser configurations and providing representative load profiles for a preliminary estimation of degradation. Firstly, synthetic wind signal generation (Section 2.1) is combined with low-order wind turbine modelling to calculate output power (Section 2.2). Moreover, we examine the additional impact of aggregate power filtering (Section 2.3), resulting from the geographical dispersion of turbines in wind parks. The Wunsiedel electrolysis plant in Northern Bavaria is used as a case study to evaluate its energy utilisation and hydrogen production, when directly coupled with a wind power source (Section 2.4). Several use cases have been introduced in this study that relate stack operation to electrolysis plant power input:

https://doi.org/10.52202/077185-0072

1. Effect of average wind speed (Section 3.1)
2. Effect of coupling with a wind park, consisting of 10 turbines (Section 3.2)
3. Effect of modular (1, 2 or 4 independent modules) configuration (Section 3.3)
4. Effect of electrolyser capacity (50% or 100% of wind power plant capacity), (Section 3.4)

2 MODEL DESCRIPTION

2.1 Wind characterisation

Wind speed can be characterised over time through the Van der Hoven model (Burton 2011). In the turbulent region, which corresponds to timescales of less than 10 to 15 minutes (Rose and Apt 2012), there is a number of mathematical models to describe high frequency wind behaviour, like the Kaimal, von Karman and Mann spectra (Jonkman 2009; Burton 2011).

In this analysis, synthetic wind speed profiles are generated using the open-source software TurbSim® developed by NREL (Jonkman, 2009). Among the vast range of modelling options, Kaimal representation, according to the IEC standard (IEC 61400-1, 2005) is selected. Subsequently, stochastic wind signals for the longitudinal direction are extracted based on the Veers method described in (Veers, 1988; Rose and Apt, 2012). The input parameters for this method are the mean wind speed, the turbulence characteristic category (A,B,C) and the turbulence type (Normal or Extreme turbulence). Wind turbulence is in principle attributed to flow disturbances and thermal effects caused by local topological characteristics (Burton, 2011), which means that these parameters are location – specific.

Two different wind speed scenarios are examined in this study (Figure 2):

(a) High turbulence: 8 m/s average wind speed
(b) High turbulence: 12 m/s average wind speed

Generated 15-minute wind signals, with this method are not capturing extreme events, such as gusts, which have been investigated by other studies (Anvari *et al.*, 2016; Bierbooms 2009)

2.2 Wind turbine model

The power generation of a wind turbine is simulated through a commercially available MATLAB model (MathWorks). This is a low-order, transient turbine model with 1 s time resolution, that simulates the coupling between the generator and the turbine as a rigid body. Thus, according to the rotational form of Newton's second law, the system state equation is:

$$J_{\mathrm{eq}}\dot{\omega} = T_{WT} - T_G. \quad (1)$$

Similar simulation schemes are described by Hoffmann (2002), Kumar and Chatterjee (2016), and Pathmanathan and Ertugrul (2009).

The WindPACT reference 3 MW wind turbine (Rinker and Dykes, 2018) is used as a case study in this analysis. To determine rotor inertia, Gonzalez-Rodriguez *et al.* (2023) proposed a methodology that considers blade geometry and centre of gravity position. The power coefficient-tip speed ratio relationship $cp(\lambda)$ is estimated using the formula described in Slootweg *et al.* (2005). The equivalent rotational inertia can be calculated from the following equation, which contains both the rotor inertia J_{WT} and generator inertia J_G , scaled by the gearbox ratio *GB* of the transmission system (MathWorks):

$$J_{eq} = J_{WT} + J_G GB^2 = 2.116\text{e}7 \text{ kg m}^2. \quad (2)$$

Regarding wind turbine operation, two different control modes are modelled: rotating speed control below the rated wind speed (operating region 2 in Figure 1) and blade pitch control above it (operating region 3 in Figure 1). Rotating speed is controlled based on the Optimal Torque concept, where operation is determined by the following Maximum Power Point Tracking characteristic curve (Kumar and Chatterjee, 2016):

$$T_{opt} = \frac{1}{2}\rho_{air}\pi R^5 \frac{C_p^{max}}{\lambda_{opt}^3}\omega^2 = K_{opt}\omega^2 \quad (3)$$

https://doi.org/10.52202/077185-0072

The optimal operation coefficient K_{opt} is constant and defined explicitly by the blade characteristics (radius R, optimum tip speed ratio λ_{opt}, maximum power coefficient c_p^{max}) and air density ρ_{air}.

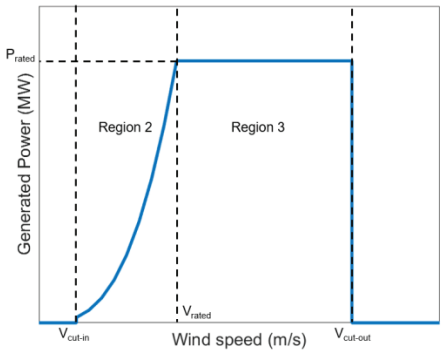

Figure 1: Wind turbine power curve, according to Kumar and Chatterjee (2016)

Furthermore, pitch angle control is adjusted according to the P-control scheme and parameters presented in Slootweg *et al.* (2005). Power losses are not considered in this analysis. The diagrams in Figure 2 demonstrate the power generation response to a wind speed input signal, either below or slightly above the rated wind speed value of 11.8 m/s. In accordance with observations made by Apt (2007), the wind turbine inertial characteristics play a considerable role in the filtering of high frequency wind fluctuations. Meanwhile, in operation above rated wind speed, generated power remains at its nominal value, using blade pitch angle control.

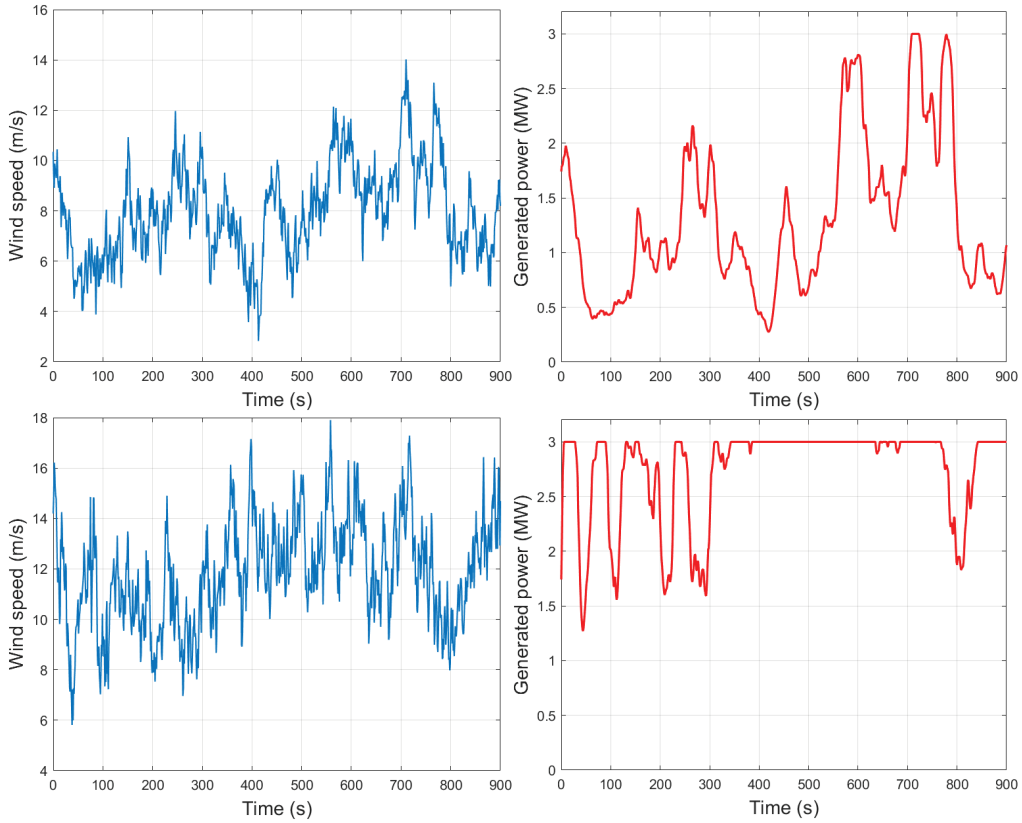

Figure 2: Wind speed (left) and generated power of the wind turbine (right) at 8 m/s (top) and 12 m/s (bottom) average wind speed

https://doi.org/10.52202/077185-0072

2.3 Geographical smoothing

Several researchers have investigated the topic of aggregate power output generated by wind parks and there is a wide consensus about the presented smoothing effect (Nanahara *et al.,* 2004; Naemi and Brear, 2020, Yang *et al.,* 2020; Meglic and Goic, 2022). Even within a wind park, spatially dispersed turbines present a level of coherence close to zero, regarding their power output on high frequencies. This becomes evident in the total power output of a wind park which approaches the scenario of totally uncorrelated wind turbines, at frequencies higher than 3 mHz (Naemi and Brear, 2020). Nanahara *et al.* (2004) investigated wind speed coherence across different measurement sites and proposed a correlation for its calculation. Its parameters are location-specific and vary over the year. The authors calculate the wind park power output using an equivalent low-pass filter (Figure 3 - left) applied to the output of a single, typical wind turbine. Even though the filter gain diagram varies with coherence, all investigated cases converged to the turbine number square root limit at the high frequency region. A similar convergence limit is observed by (Naemi and Brear 2020), which is equivalent to the assumption of Gaussian independence among the wind turbines.

This filtering methodology can be applied to specific wind parks, with a given number of wind turbines and geographical dispersion, allowing for a preliminary estimation on aggregate power smoothing. However, further research is necessary to establish parameters relevant to local topography and the effects of wake interaction within a wind park (González-Longatt *et al.,* 2012). In this study the equivalent filter values described by Nanahara *et al.* (2004) are used for a wind park comprising 10 turbines. The influence of the two extreme scenarios: low coherence (maximum filtering effect) and high coherence is demonstrated in Figure 3.

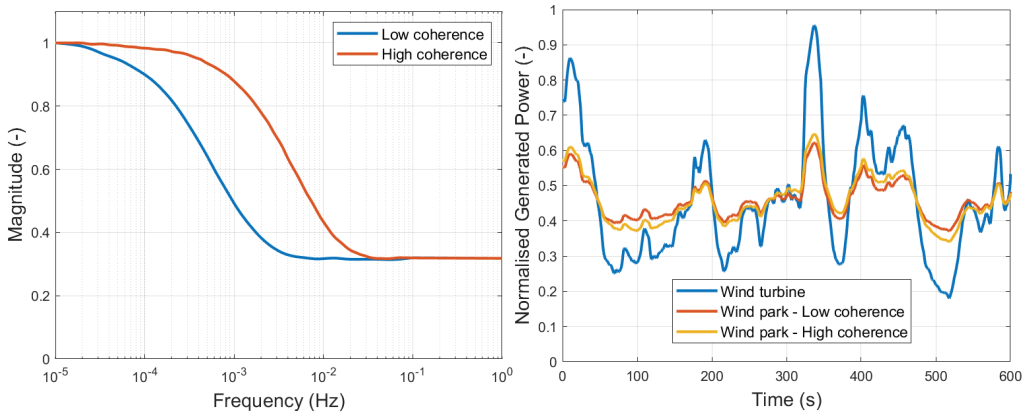

Figure 3: Filter magnitude (left) as presented in (Nanahara et al., 2004) and application to output power (right)

It can be concluded that there is a considerable reduction in relative fluctuation magnitude after applying the low-pass filters. However, the difference between these two extreme scenarios is relatively low and thus only the low coherence case is used for further analysis in this study.

2.4 Electrolyser system description

The specifications of the electrolysis plant located at the Wunsiedel Energy Park in Northern Bavaria; Germany are used as theoretical case study in this work. It is a PEM electrolyser of the Siemens Silyzer 300 series, with a nominal capacity of 8.75 MW. It consists of twelve electrolysis stacks divided equally into two modules, which can be operated independently. The technical specifications according to the manufacturer are listed in Table 1:

https://doi.org/10.52202/077185-0072

Table 1: Siemens Silyzer 300 specifications (Siemens Energy)

Electrolyser model	Siemens Silyzer 300
Nominal electrical power	8.75 MW
Module minimum load	40 %
Module ramp rate	10 %/s
Warm startup time	60 s

3 CASE STUDIES & RESULTS

In this study, a direct coupling between the electrolyser and the wind turbines is considered direct, omitting the buffering effect of any energy storage systems. The wind park provides the complete input power for the electrolyser. The operation of the electrolyser focuses on maximum hydrogen production and thus maximum energy consumption, while excess power is dispatched to the grid. All use cases are compared by means of their respective hydrogen production and energy utilisation rate (Figure 9), which is defined as the ratio of utilised to supplied energy. The calculation of hydrogen production is based on the polarisation curve provided by Järvinen *et al.* (2022), for an experimental PEM electrolysis cell kept at 75° C and operational range up to 1.8 A/cm^2. Voltage efficiency is defined according to Lettenmeier (2021) in terms of the higher heating value. Furthermore, faradaic efficiency for ambient pressure operation is derived from experimental data in Yodwong *et al.* (2020). Hydrogen production rate $\dot{m}_{H2}$ is correlated to the cell input power P_{in} and total efficiency η_{cell}, which is the product of its faradaic η_f and voltage efficiency η_v, by the following equation (Antoniou *et al.*, 2024):

$$\eta_{cell} = \eta_v \eta_f = \frac{\dot{m}_{H2} C_{H2}}{P_{in}}. \quad (4)$$

Hydrogen production is scaled to the rated wind source capacity, in order to enable direct comparison between all the use studies and the case where the electrolysis plant is coupled with a wind park, consisting of ten turbines (Section 3.2).

Regarding the operating strategy, split range control of the electrolyser is assumed to follow a type of "last in-first out" approach, where operation of the first module is prioritised as power input increases. At the base case of 2 modules for example, upon reaching the 40 % threshold (Table 2), the second module is activated and load is distributed equally. During its 60 s startup delay, the first module utilises the respectable load up to its operating range:

Table 2: Electrolyser operating strategy at base case (2 modules)

Input power	Load distribution
0% – 20%	[0 | 0]
20% – 40%	[P | 0]
40% – 100%	[P/2 | P/2]

3.1 Effect of average wind speed

In the first case, the electrolyser is assumed to have capacity equal to the nominal capacity of the single wind turbine, which is described in section 2.2. Two different scenarios are examined with average wind speeds below and above the rated wind speed to demonstrate the contrast in the wind turbine operating regimes. Figure 4 illustrates the electrolyser power input and load for each module, scaled at the rated electrolyser capacity. Both electrolyser modules are in operation at the beginning of the investigated time period. As it can be seen in Figure 4 (left), on-off operation at lower wind speeds is heavily affecting load following capability, due to the 60 s delay at startup. As long as the modules are in operation, the input load fluctuations are captured efficiently. In Figure 4 (right), wind speeds above the turbine rated speed lead to steady operation periods and total energy utilisation reaches 100 %.

https://doi.org/10.52202/077185-0072

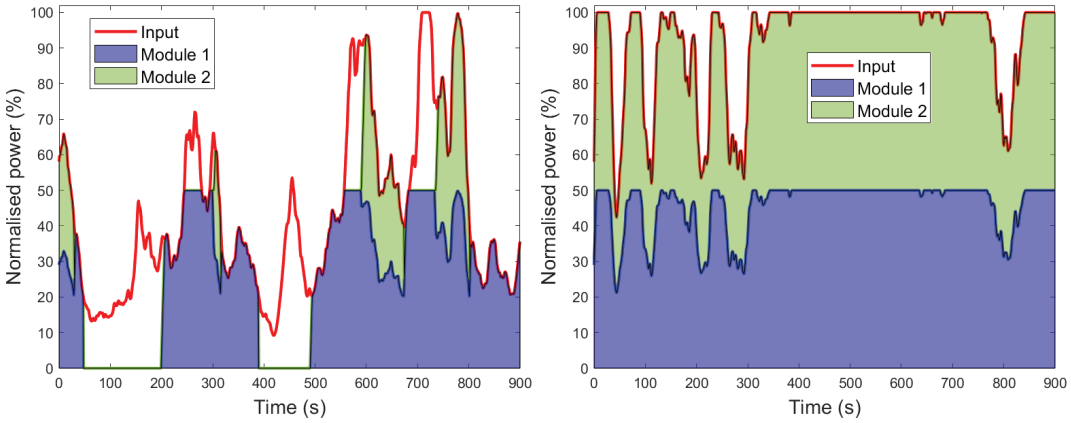

Figure 4: Electrolyser (2 modules) operating at wind power input for 8 m/s (left) and 12 m/s (right) average wind speed

3.2 Effect of wind park filtering

In this case, electrolyser capacity is scaled to 100 % of the nominal power of a wind park consisting of ten wind turbines, with aggregate output characteristics similar to the specific plant presented in section 2.3. In comparison with the previous case in section 3.1, the filtered load leads to fluctuations of lower magnitude and to a higher power utilisation from the electrolyser, caused by the reduced number of shutdowns as shown in Figure 5 (left). At higher wind speeds in Figure 5 (right), predominantly steady operation at full load is achieved for both modules.

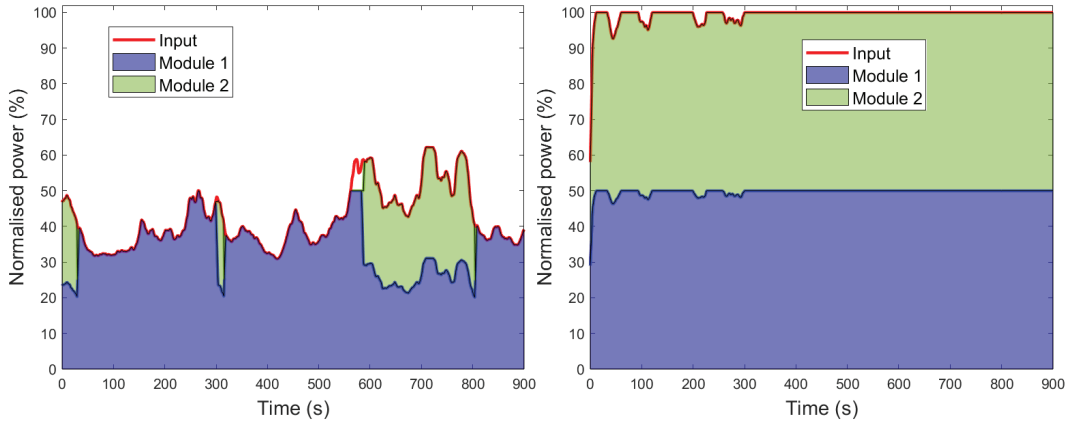

Figure 5: Electrolyser (2 modules) operating under power input by a wind park of ten wind turbines at 8 m/s (left) and 12 m/s (right) wind speed

3.3 Effect of module number

Two additional cases are examined, considering one (Figure 6) and four (Figure 7) independent modules with similar specifications and operating strategies, subject to the same load profiles, like the base case of 2 modules (Section 3.1). Target is to demonstrate the system design sensitivity to modularisation in the case of reducing and increasing their number by a factor of 2. It can be concluded that an increased number of modules can contribute to better energy utilisation and a higher hydrogen production, as other studies remark, e.g. Lange *et al.* (2023), mainly because the minimum operation threshold of the entire plant gets lower. Electrolyser operation in a single module, leads to underutilisation of input energy, due to the limited operational range. On the other hand, operation above rated wind speed is efficiently capturing power fluctuations, as long as it operates without any shutdown events.

https://doi.org/10.52202/077185-0072

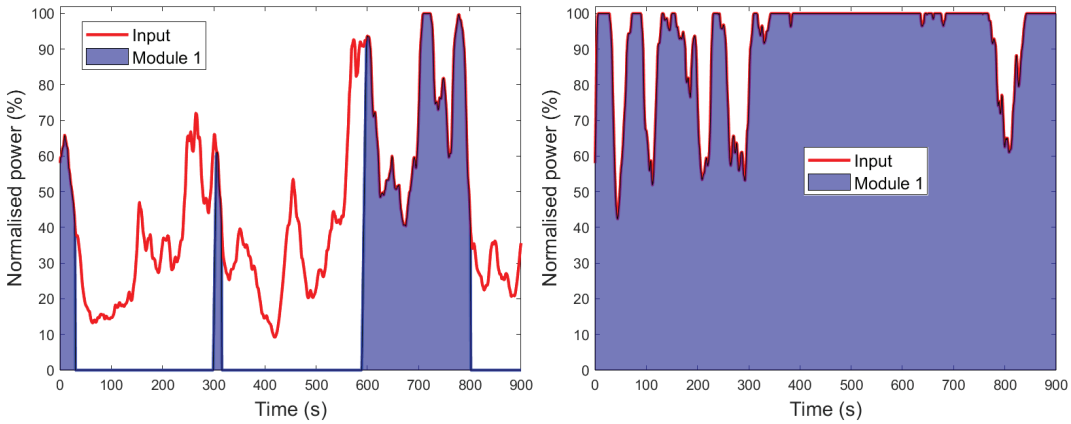

Figure 6: Electrolyser (1 module) operating under power input of 8 m/s (left) and 12 m/s (right) wind speed

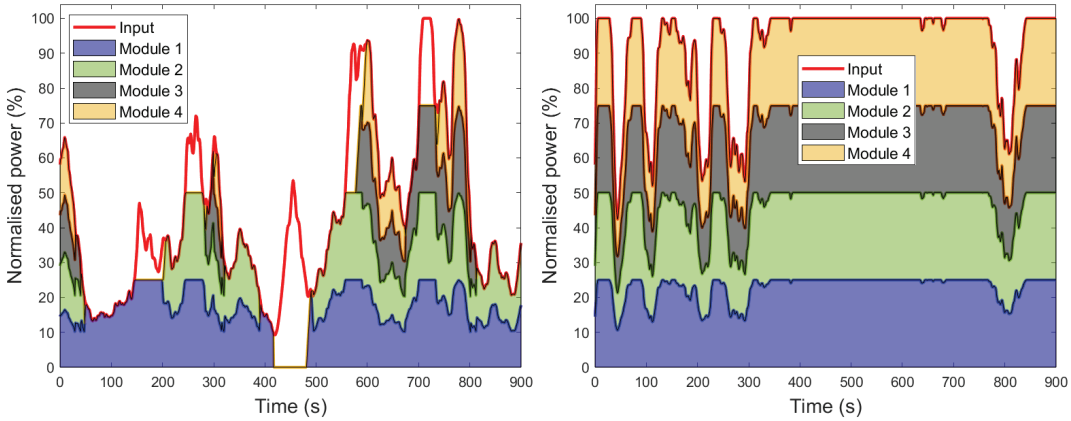

Figure 7: Electrolyser (4 modules) operating under power input of 8 m/s (left) and 12 m/s (right) wind speed

3.4 Effect of electrolyser capacity

In this case (Figure 8), the rated electrolyser capacity is dimensioned at 50 % of the nominal power of the single wind turbine. This value is comparable with other studies (Hassan *et al.,* 2023 and Hofrichter *et al.,* 2023) that have examined the optimal electrolyser-to-wind source capacity ratio in actual use cases. At lower wind speeds, as depicted in Figure 8 (left), utilisation is sufficiently high, mainly because of the lower activation threshold and less shutdowns. However, only 15 % more energy utilisation is achieved, and 17% more hydrogen is produced, in comparison with the 4-modules case (Figure 7 - left). In Figure 8 (right) it can also be observed, that at higher wind speeds hydrogen production is almost halved, compared with the full capacity case, while electrolyser operation exhibits a nearly steady profile. On that account, the sizing of the electrolyser capacity depends strongly on the expected performance of the coupled wind plant and can thus be preliminarily estimated using the annual, location-specific wind data.

https://doi.org/10.52202/077185-0072

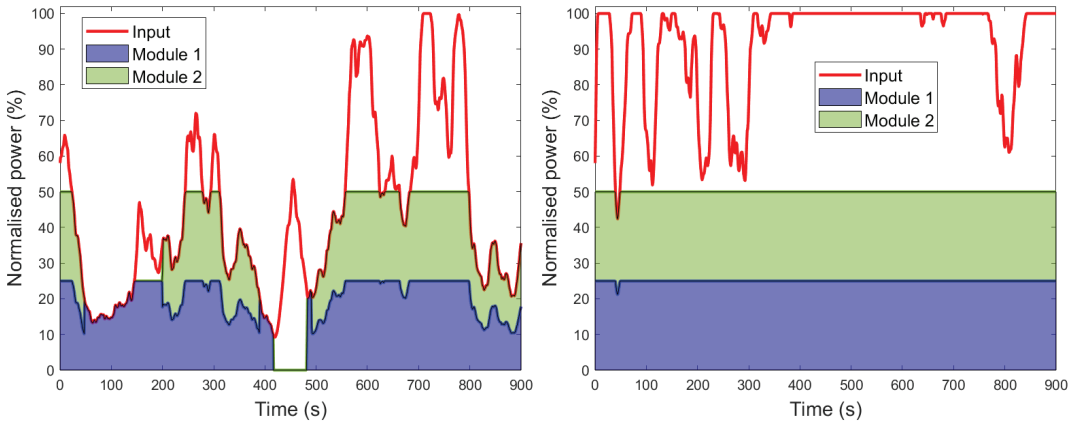

Figure 8: Electrolyser (2 modules), scaled at 50% of wind power plant, operating under power input of 8m/s (left) and 12m/s (right) wind speed

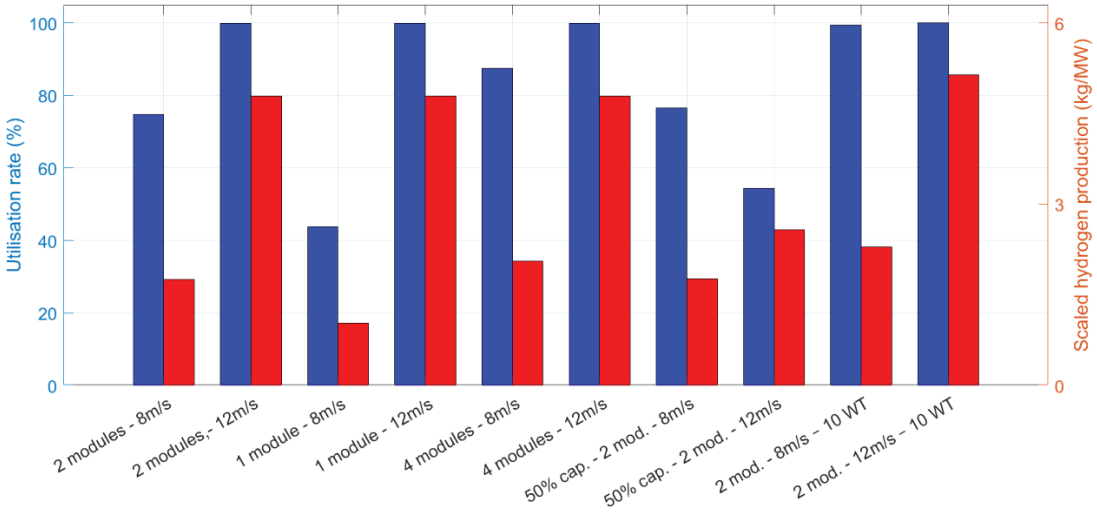

Figure 9: Utilisation rate and hydrogen production in all use cases

4 CONCLUSIONS

This work demonstrates the impact of volatility on the operation of a PEM electrolyser system that is directly coupled with a wind power source. Firstly, it has been estimated how primary wind speed fluctuations are filtered at high frequencies by wind turbines. Additionally, the geographical dispersion of wind turbines within a wind park has been considered, resulting in further aggregate power output filtering. In conclusion, power volatility is influenced not only by wind characteristics, such as wind speed and turbulence intensity, but also by wind turbine inertia and its applied control systems, as well as geographical distribution and site-specific wind behaviour inside a power plant. The case study presented here is based on the specifications of the PEM electrolysis plant located at the Wunsiedel Energy Park in Northern Bavaria, Germany. Several modular configuration and rated capacity cases operating under different load profiles have been investigated.

Technical specifications are shown to affect the electrolyser energy utilisation capability and hydrogen production. In particular, the minimum operating threshold and warm startup time play a major role in the electrolyser operation. However, the nominal ramp rate of 10 %/s was deemed as sufficient to capture all input power fluctuations, that exhibited lower speeds. Furthermore, using a higher number of independent modules provides increased uptime and hydrogen production, mainly due to fewer

https://doi.org/10.52202/077185-0072

shutdowns and faster activation. Module number dimensioning should be evaluated on the electrolysis plant level, to determine whether enhanced performance outweighs the increased system complexity. The modular configuration can nevertheless be further optimised in terms of operating strategy and power input allocation. Capacity dimensioning of the electrolyser has been examined in two cases: 100 % and 50 % of the nominal capacity in the wind power source. At high wind speed levels, halving electrolyser capacity leads to a considerable decrease in produced hydrogen and overall energy utilization. However, at low wind speed operation this difference is negligible. It is thus evident, that there is a lot of potential for rated capacity optimisation, taking into consideration further techno-economic criteria.

Overall, this study establishes a framework base for the dimensioning of an electrolyser under dynamic operation. A wide selection of the conditions and limitations in coupling the electrolyser with wind power sources has been addressed and future work will concentrate on the optimisation of the electrolyser capacity, modular configuration and operating strategy, considering cumulative degradation and techno-economic parameters.

NOMENCLATURE

cp	Power coefficient	(-)
C_{H2}	Hydrogen energy density	(J/kg)
GB	Gearbox ratio	(-)
J	Moment of inertia	($kg \cdot m^2$)
$\dot{m}_{H2}$	Hydrogen production rate	(kg/s)
P	Power	(W)
R	Blade radius	(m)
T	Torque	(N·m)
η	Efficiency	(-)
λ	Tip-speed ratio	(-)
ρ	Density	(kg/m^3)
ω	Rotational speed	(rad/s)

Subscript

eq	equivalent
f	faradaic
G	generator
opt	optimal
v	Voltage
WT	wind turbine

REFERENCES

Ajanovic, A., Sayer, M., Haas, R., 2024, On the future relevance of green hydrogen in Europe, *Appl. Energ.*, vol. 358, 122586.

Antoniou, A., Celis, C., Mas, R., Berastain, A., Xiros, N., Papageorgiou, G., Maimaris, A., Wang, T., 2024, Effective thermal-electric control system for hydrogen production based on renewable solar energy, *Int. J. Hydrogen Energ.*, vol. 53, no. 75: p. 173–183.

Anvari, M., Lohmann, G., Wächter, M., Milan, P., Lorenz, E., Heinemann, D., Tabar, M.R.R., Peinke, J., 2016, Short term fluctuations of wind and solar power systems, *New J. Phys.*, vol. 18, no. 6, 63027.

Apt, J., 2007, The spectrum of power from wind turbines, *J. Power Sources*, vol. 169, no. 2: p. 369–374.

Barreda, N., 2023, *Impact-Assessment-on-the-RED-II-DAs*, Hydrogen Europe.

Bierbooms, W., 2009, Application of Constrained Stochastic Simulation to Determine the Extreme Loads of Wind Turbines, *Wind Energ.*, vol. 131, no. 3: p. 207.

https://doi.org/10.52202/077185-0072

Bundesnetzagentur, 2022, Monitoringbericht 2022.
Burton, T., 2011, *Wind energy handbook,* 2nd ed., Wiley, Chichester, West Sussex, England, 742 p.
Cooper, N., Horend, C., Röben, F., Bardow, A., Shah, N., 2022, A framework for the design & operation of a large-scale wind-powered hydrogen electrolyzer hub, *Int. J. Hydrogen Energ.*, vol. 47, no. 14: p. 8671–8686.
Egeland-Eriksen, T., Jensen, J.F., Ulleberg, Ø., Sartori, S., 2023, Simulating offshore hydrogen production via PEM electrolysis using real power production data from a 2.3 MW floating offshore wind turbine, *Int. J. Hydrogen Energ.*, vol. 48, no. 74: p. 28712–28732.
European Commission, 2019, *The European Green Deal* [online], Available from: https://commission.europa.eu/strategy-and-policy/priorities-2019-2024/european-green-deal_en.
European Commission, 2023, *Commission Delegated Regulation (EU) supplementing Directive (EU) 2018/2001 of the European Parliament and of the Council by establishing a Union methodology setting out detailed rules for the production of renewable liquid and gaseous transport fuels of non-biological origin*, 13 p.
Fang, R. and Liang, Y., 2019, Control strategy of electrolyzer in a wind-hydrogen system considering the constraints of switching times, *Int. J. Hydrogen Energ.*, vol. 44, no. 46: p. 25104–25111.
González-Longatt, F., Wall, P., Terzija, V., 2012, Wake effect in wind farm performance: Steady-state and dynamic behavior, *Renewable Energy*, vol. 39, no. 1: p. 329–338.
Gonzalez-Rodriguez, A.G., Roldan-Fernandez, J.M., Nieto-Nieto, L.M., 2023, Unveiling Inertia Constants by Exploring Mass Distribution in Wind Turbine Blades and Review of the Drive Train Parameters, *Machines*, vol. 11, no. 9: p. 908.
Hassan, Q., Sameen, A.Z., Salman, H.M., Jaszczur, M., 2023, Large-scale green hydrogen production via alkaline water electrolysis using solar and wind energy, *Int. J. Hydrogen Energ.*, vol. 48, no. 88: p. 34299–34315.
Hoffmann, R., 2002, *A comparison of control concepts for wind turbines in terms of energy capture*: PhD Thesis, Technische Universität Darmstadt.
Hofrichter, A., Rank, D., Heberl, M., Sterner, M., 2023, Determination of the optimal power ratio between electrolysis and renewable energy to investigate the effects on the hydrogen production costs, *Int. J. Hydrogen Energ.*, vol. 48, no. 5: p. 1651–1663.
International Electrotechnical Commission, 2005, *Wind turbines-Part 1: Design requirements,* 3rd ed., Geneva, Switzerland, no. IEC 61400-1.
Järvinen, L., Puranen, P., Kosonen, A., Ruuskanen, V., Ahola, J., Kauranen, P., Hehemann, M., 2022, Automized parametrization of PEM and alkaline water electrolyzer polarisation curves, *Int. J. Hydrogen Energ.*, vol. 47, no. 75: p. 31985–32003.
Jonkman, B.J., 2009, TurbSim User's Guide: Version 1.50.
Kojima, H., Nagasawa, K., Todoroki, N., Ito, Y., Matsui, T., Nakajima, R., 2023, Influence of renewable energy power fluctuations on water electrolysis for green hydrogen production, *Int. J. Hydrogen Energ.*, vol. 48, no. 12: p. 4572–4593.
Kumar, D. and Chatterjee, K., 2016, A review of conventional and advanced MPPT algorithms for wind energy systems, *Renew. Sust. Energ. Rev.*, vol. 55: p. 957–970.
Lange, H., Klose, A., Lippmann, W., Urbas, L., 2023, Technical evaluation of the flexibility of water electrolysis systems to increase energy flexibility: A review, *Int. J. Hydrogen Energ.*, vol. 48, no. 42: p. 15771–15783.
Lettenmeier, P., 2021, *Efficiency-White-paper*, Siemens Energy.
Lu, X., Du, B., Zhou, S., Zhu, W., Li, Y., Yang, Y., Xie, C., Zhao, B., Zhang, L., Song, J., Deng, Z., 2023, Optimization of power allocation for wind-hydrogen system multi-stack PEM water electrolyzer considering degradation conditions, *Int. J. Hydrogen Energ.*, vol. 48, no. 15: p. 5850–5872.
Maggio, G., Nicita, A., Squadrito, G., 2019, How the hydrogen production from RES could change energy and fuel markets: A review of recent literature, *Int. J. Hydrogen Energ.*, vol. 44, no. 23: p. 11371–11384.

https://doi.org/10.52202/077185-0072

MathWorks, *Control Design for Wind Turbine* [online], Available from: https://uk.mathworks.com/help/control/ug/wind-turbine-control-design.html#mw_rtc_ControlDesignForWindTurbineExample_M_A6F45497.

Meglic, A. and Goic, R., 2022, Impact of Time Resolution on Curtailment Losses in Hybrid Wind-Solar PV Plants, *Energies*, vol. 15, no. 16, 5968.

Mucci, S., Mitsos, A., Bongartz, D., 2023, Power-to-X processes based on PEM water electrolyzers: A review of process integration and flexible operation, *Comp. Chem. Eng.*, vol. 175, no. 14, 108260.

Naemi, M. and Brear, M.J., 2020, A hierarchical, physical and data-driven approach to wind farm modelling, *Renewable Energy*, vol. 162, no. 6: p. 1195–1207.

Nanahara, T., Asari, M., Sato, T., Yamaguchi, K., Shibata, M., Maejima, T., 2004, Smoothing effects of distributed wind turbines. Part 1. Coherence and smoothing effects at a wind farm, *Wind Energy*, vol. 7, no. 2: p. 61–74.

Rinker, J. and Dykes, K., 2018, WindPACT Reference Wind Turbines.

Rose, S. and Apt, J., 2012, Generating wind time series as a hybrid of measured and simulated data, *Wind Energy*, vol. 15, no. 5: p. 699–715.

Sarrias-Mena, R., Fernández-Ramírez, L.M., García-Vázquez, C.A., Jurado, F., 2015, Electrolyzer models for hydrogen production from wind energy systems, *Int. J. Hydrogen Energ.*, vol. 40, no. 7: p. 2927–2938.

Schnuelle, C., Wassermann, T., Fuhrlaender, D., Zondervan, E., 2020, Dynamic hydrogen production from PV & wind direct electricity supply – Modeling and techno-economic assessment, *Int. J. Hydrogen Energ.*, vol. 45, no. 55: p. 29938–29952.

Siemens Energy, *Datasheeet PEM Electrolyzer 17.5 MW* [online]. Available from: https://assets.siemens-energy.com/siemens/assets/api/uuid:40d117f9-1b4f-4816-ae58-b47cf011d406/datasheet-pem-electrolyzer-17-5mw.pdf.

Slootweg, J.G., Polinder H., Kling W. L., 2005, Reduced-order Modelling of Wind Turbines, *In:* Ackermann, Thomas, *Wind Power in Power Systems*, John Wiley & Sons, Chichester, West Sussex, England, p. 555-586.

Terlouw, T., Bauer, C., McKenna, R., Mazzotti, M., 2022, Large-scale hydrogen production via water electrolysis: a techno-economic and environmental assessment, *Energy Environ. Sci.*, vol. 15, no. 9: p. 3583–3602.

Tully, Z., Starke, G., Johnson, K., King, J., 2023, *An Investigation of Heuristic Control Strategies for Multi-Electrolyzer Wind-Hydrogen Systems Considering Degradation*.

Veers, P.S., 1988, *Three-dimensional wind simulation*, Sandia National Laboratories.

Yang, M., Zhang, L., Cui, Y., Zhou, Y., Chen, Y., Yan, G., 2020, Investigating the Wind Power Smoothing Effect Using Set Pair Analysis, *IEEE Trans. Sustain. Energy*, vol. 11, no. 3: p. 1161–1172.

Yodwong, B., Guilbert, D., Phattanasak, M., Kaewmanee, W., Hinaje, M., Vitale, G., 2020, Faraday's Efficiency Modeling of a Proton Exchange Membrane Electrolyzer Based on Experimental Data, *Energies*, vol. 13, no. 18, 4792.

ACKNOWLEDGEMENT

The authors acknowledge funding by the Bundesministerium für Bildung und Forschung (BMBF, Federal Ministry of Education and Research) within the project "Modellentwicklung zur Steigerung der Effizienz von Elektrolyseanlagen" (HYER - Modeling of electrolysis plant to inform improved electrolyser efficiencies) (01DM22003A) and support by the Oberfrankenstiftung (Upper Franconia Foundation) within the project "ZET-Reallabor Energiezukunft Wunsiedel".

https://doi.org/10.52202/077185-0072